Environ. Sci. Technol. 1992, 26, 734-738

Radon-222 as a Groundwater Tracer. A Laboratory Study

Eduard Hoehn,*,† Hans R. von Gunten,†,‡ Fritz Stauffer,§ and Themistocles Dracos§

Paul Scherrer Institut, 5232 Villigen PSI, Switzerland, Laboratorium für Radiochemie, Universität Bern, 3000 Bern 9, Switzerland, and Institute of Hydromechanics and Water Resources Management, Swiss Federal Institute of Technology, 8093 Zurich, Switzerland

■ Radon-222 (^{222}Rn; half-life 3.8 days) was used in a laboratory study for determining residence times and velocities of water flowing through an open-topped sand box. The quartz sand in the box contained natural trace amounts of ^{226}Ra, the progenitor of ^{222}Rn. The radon method is based on the increase of the activity of ^{222}Rn in interstitial water with increasing residence time and assumes that the ingrowth can be described by the first-order kinetics of secular radioactive equilibrium. The validity of this assumption was checked in two experiments. The results of the experiments showed (a) that the ingrowth of radon in a flowing water system can be adequately described and (b) that the radon method might also be applied to field studies in sandy aquifers with groundwaters of a relatively slow flow velocity, i.e., ≥0.2 m day^{-1}. Spatial differences in the radon production were observed and explained by a model of inhomogeneous distribution of ^{226}Ra in the sand. Spatially different steady-state activities were used in the calculations which matched the observed data of the first three outlets slightly better than the first-order ingrowth approach.

Introduction

Recently we have demonstrated a new method for the determination of groundwater residence times (<15 days) and corresponding flow velocities (*1*). The basic assumption of this method is an ingrowth of the radon isotope ^{222}Rn in infiltrated groundwater from its progenitor ^{226}Ra to reach a steady-state condition according to the laws of radioactive equilibrium, recoil diffusion out of the solid phase, and losses across the water–air interface. The α-particle decay of ^{226}Ra produces ^{222}Rn, which emanates from mineral surfaces and dissolves in the water phase. Radon is a noble gas and behaves as a conservative tracer. Due to its half-life of 3.8 days, residence times of the groundwater of up to ~15 days (~4 half-lives) can be calculated from the radon activity.

During the infiltration of surface water, which has a low radon activity, radon starts to grow as the water moves in the aquifer and reaches 99% of the steady state within 25 days. A practical application of the radon method for dating is only feasible if several assumptions are valid (*1*). The following among them are of relevance for the present study: (a) The average distribution of ^{226}Ra in the studied solid materials is homogeneous on a scale which is large compared to local inhomogeneities; (b) the steady-state radon activities corresponding to residence times of the groundwater of ≥15 days are representative for the entire water flow path; and (c) losses of radon from the saturated to the unsaturated zone and to the atmosphere are constant with time (*1*).

In our previous study (*1*) we used the ingrowth of ^{222}Rn to estimate residence times of groundwaters after the infiltration of river water to aquifers of coarse and previous granular material of the perialpine belt of Switzerland. At groundwater flow velocities of 4–5 m day^{-1}, the ingrowth of radon can be observed at distances of up to 100 m. The determination of groundwater residence times is of importance for drinking-water management.

Here we describe the results of a laboratory study which tested the basic assumptions of the radon method. The advantage of a laboratory experiment over a field study is the better control of initial and boundary conditions and the possibility of checking the results by other methods. Furthermore, the grain size, the effective porosity of the sand, and the flow conditions in the box experiment were found to be similar to those of a field experiment in Canada [Chalk River (*2*)], where the mobility of radionuclides was studied over 4 days in a sandy aquifer of felspars and quartz. We wanted to determine whether the radon method was also suitable for aquifers of this type.

Table I. Parameters of the Coarser Sand Layer in the Box[a]

thickness, m	0.66
median grain size (±SD), mm	0.42 ± 0.20[b]
hydraulic conductivity, mm s^{-1}	0.73
effective porosity	0.39

[a] Reference 9. [b] Grain-size distribution; see Table IV.

Experimental Section

Apparatus. The ingrowth of radon in interstitial water was observed in a narrow open-topped sand box (Figure 1). The box contains 82 outlets, arranged along the side, for sampling and for the measurement of specific electric conductivity of the water. The outlets sample the water in the middle of the box (y-axis) to minimize wall effects. For the radon measurements, seven of eight outlets were used, located in a row 0.40 m above the bottom of the box. A few measurements of the vertical distribution of radon were made from outlets 4a and 4b located at a distance of 2.7 m from the inflow boundary. The box and the data acquisition system are described in detail in ref 3.

The box had previously been used for two-dimensional transport investigations. For these earlier experiments, it was filled with two horizontal layers differing in grain size, of well-sorted natural quartz sands of a technical grade (Zimmerli AG, Zürich, Switzerland; Table I). In the present study, we extracted water from the lower layer of coarser grains only in order to minimize outgassing of radon to the atmosphere. The parameters given in Table I for this sand layer refer to saturated conditions. The quartz sand contained <1 wt % impurities of other minerals (supplier's specifications). For our experiments, the box was operated under saturated flow conditions.

Radon Measurements. A piston pump allowed tap water to flow horizontally through the box. The water entered the box at four inlets at one end. The radon activity of the inflowing water was 0.11 Bq dm^{-3}. After diversion by separation devices (see Figure 1), the water flowed parallel to the walls. Near the discharge end, a sieve separated the quartz sand from a container out of which water was pumped. Our study consisted of two experiments: (i) measurement of the radon activity as a function

† Paul Scherrer Institut.
‡ Universität Bern.
§ Swiss Federal Institute of Technology.

0013-936X/92/0926-0734$03.00/0

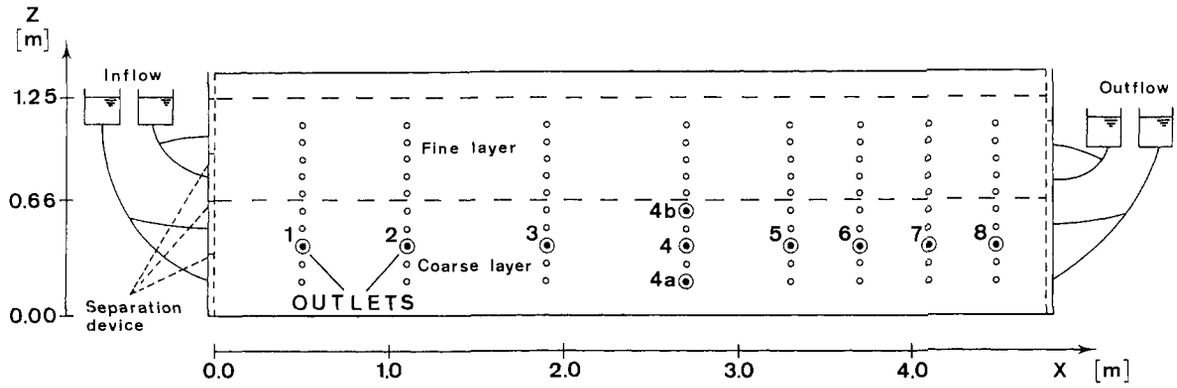

Figure 1. Experimental installation, slightly modified from ref 3: length (x-axis) 4.8 m, width (y-axis) 0.05 m, height (z-axis) 1.4 m; separation devices homogenize inflow.

of time and distance under constant-flow conditions and (ii) investigation of the radon activity in the box after steady state was reached with the progenitor, ^{226}Ra (no water flow). The experiments are interpreted with the law of radioactive decay in which the ingrowth of a daughter from its parent is described as

$$A_t = A_e[1 - \exp(-\lambda t)] \quad (1)$$

A_t and A_e are the activities of ^{222}Rn at time t and at steady state with ^{226}Ra, respectively, and $\lambda = 0.18$ day^{-1} is the radioactive decay constant of ^{222}Rn. The activity is proportional to the concentration ($A_x = \lambda N_x$, where N_x is the number of atoms of the nuclide x). In eq 1, t represents the time elapsed between the entrance of the water into the box and the sampling at the respective outlet. It is assumed to correspond to the mean residence time of the water in the box.

During experiment i, samples were taken on the same day from three separated outlets. Separated outlets were selected to minimize interferences by sampling. For this experiment, water flowed at a constant rate of 6.30 ± 0.03 cm^3 min^{-1}. Darcy's law relates the pore velocity at constant discharge rate linearly to the medium's hydraulic conductivity, the hydraulic gradient, and the effective porosity. When Darcy's law is used with the parameters given in Table I, this flow rate corresponds to a residence time within the box of ~13 days. Synchronously to the start of the radon measurements, water was tagged with a step input of 200 ppm NaCl, a concentration 10 times greater than that of the tap water. The breakthrough of the NaCl solution at outlets was measured by electrical conductivity and was analyzed by assuming that the tracer represents the flow of water. The residence time of the NaCl between different outlets was compared with the radon method.

Experiment ii started when the added NaCl was completely eluted. The water supply was interrupted and the water in the box was left stagnant for ~1 month, i.e., about 8 half-lives of ^{222}Rn. Subsequent sampling revealed steady-state activities throughout the box. All outlets were sampled one to three times, leaving ample time (~1 month) between sampling for reestablishing steady-state conditions. This second experiment was necessary because the residence time of the water in the box was too short in experiment i to reach steady-state conditions for ^{222}Rn.

The withdrawal of a sample of 1 L of water, which is necessary to obtain sufficient sensitivity for the radon measurement, involved a bulk volume with a spherical radius influencing ~9 cm. While this water was replaced during flow conditions, a total of ~6% of the stagnant water was removed, during no-flow conditions. This is considered to be a slight source of error. For sampling, the outlets were connected with stainless steel capillaries

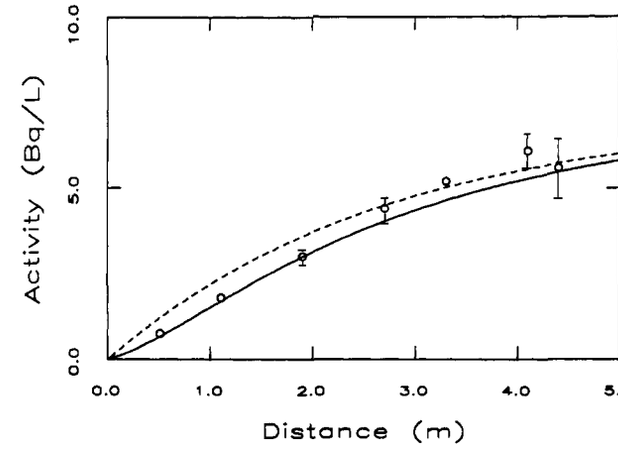

Figure 2. Mean radon activities in box at constant flow: circles, measured values (errors ±1σ); dashed line, simulated radon ingrowth, assuming homogeneous production (homogeneous distribution of ^{226}Ra; steady-state activity of ^{222}Rn 7.2 Bq dm^{-3} of water; see Table II); solid line, simulated ingrowth, assuming inhomogeneous production (inhomogeneous distribution of ^{226}Ra).

which reached to the bottom of 1-dm^3 glass cylinders containing 20 cm^3 of toluene-based liquid scintillator. Losses of radon to the atmosphere were minimized by the floating toluene layer, since the solubility of radon in toluene is ~40 times higher (*4*) than in water. The samples were prepared for liquid scintillation counting by extraction of the radon into the liquid scintillator (*4*). Sampling required 4–13 h, depending on the flow conditions at the respective outlet; the decay of radon during sampling was corrected for, and radioactive equilibrium between radon and its daughters was attained before measurement. The overall error of a single sample was estimated to be in the order of ±20%; this is based on multiple measurements of samples, extraction tests of ^{226}Ra standard solutions, and checks for Rn losses. The error includes uncertainties in sampling, in the chemical procedure, and in counting statistics.

Results and Discussion

Radon Ingrowth. In experiment i, radon was measured three times in the interstitial water of the sand box at seven outlets under steady-flow conditions. We subtracted the decay-corrected value of the initial activity (0.11 Bq dm^{-3}) from these measurements. The results are presented in Table IIa and Figure 2. Outlet 6 (see Figure 1) was clogged throughout the experiments. The mean radon activities increased with increasing flow distance from the inflow boundary, in qualitative agreement with the model. A steady state of ^{222}Rn was not reached within the box.

Table II. Radon Activities in the Water, Residence Times, and Pore Velocities

outlet	distance from inlet, m	radon activities (replicates and means), Bq dm^{-3} 1	2	3	μ	residence time,[a] days	pore velocity, m day^{-1}
				(a) Experiment i			
1	0.51	0.83	0.71	0.73	0.76 ± 0.06	0.62 ± 0.05	0.82 ± 0.05
2	1.1	1.8	1.8	1.7	1.8 ± 0.1	1.6 ± 0.09	0.69 ± 0.03
3	1.9	2.9	3.2	2.8	3.0 ± 0.2	3.0 ± 0.2	0.63 ± 0.04
4	2.7	4.4	4.7	4.2	4.4 ± 0.3	5.2 ± 0.4	0.52 ± 0.03
5	3.3	5.2	5.3	5.1	5.2 ± 0.1	7.1 ± 0.1	0.46 ± 0.01
7	4.1	6.4	5.8	6.0	6.1 ± 0.3	10.4 ± 0.5	0.39 ± 0.02
8	4.5		6.0	5.1	5.6 ± 0.6	8.3 ± 0.9	0.53 ± 0.06
mean							0.58 ± 0.15
				(b) Experiment ii			
1	0.51	5.6	4.4	5.5	5.2 ± 0.7[b]		
2	1.1	6.5			6.5 ± 1.3		
3	1.9	8.0	6.3		7.2 ± 1.2		
4	2.7	8.4	7.5	8.0	8.0 ± 0.5		
4a[c]	2.7	7.0			7.0 ± 1.4		
4b[d]	2.7	7.9			7.9 ± 1.6		
5	3.3	7.2	6.0		6.5 ± 0.8		
7	4.1	7.4	9.0	6.0	7.5 ± 1.5		
8	4.5				7.0 ± 1.4[e]		

[a] Calculated with eq 1 (A_e = 7.2 ± 0.6 Bq dm^{-3}); values corrected for A of inflowing water. [b] Value not used for calculation of A_e. [c] Distance from bottom of box, 0.6 m. [d] Distance from bottom of box, 0.2 m. [e] Value from experiment i (5.6 ± 0.6 Bq dm^{-3}) corresponding to a residence time of 9.1 days (NaCl test), extrapolated to steady state.

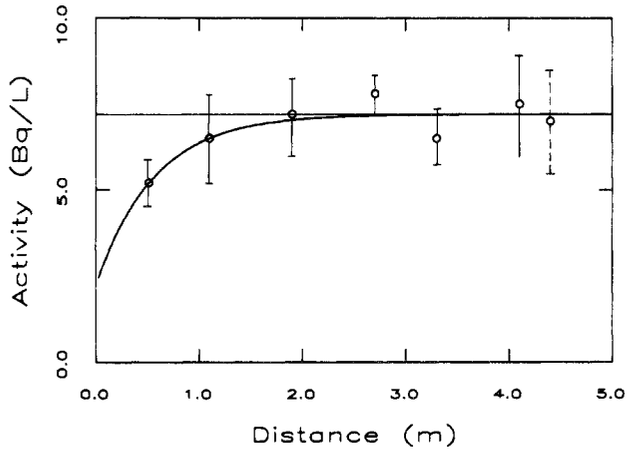

Figure 3. Mean steady-state radon activities in box (no flow for more than 1 month): circles, measured values (errors ±1σ, or ±20% for single measurement); thin line, constant value of 7.2 Bq dm^{-3} of water (see Table II); heavy line, simulated activity distribution, assuming inhomogeneous production of radon. Value at 4.5 m extrapolated from experiment i of Table II.

Radon at Steady State. Steady-state radon activities were measured in experiment ii; see Table IIb and Figure 3. The data at the different outlets scatter more than in experiment i. They agree with an expected constant activity within the accuracy of the measurements, except for the first outlet, whose steady-state value was significantly lower than the other ones. The steady-state activity of outlet 8 was not measured during experiment ii, but estimated from the radon activity of experiment i at this outlet: The residence time (9.1 days) is known from the NaCl tracer test and corresponds to ~80% of the steady state. Therefore, the value of 5.6 ± 0.6 Bq dm^{-3}, measured during experiment i was extrapolated to 7.0 ± 1.4 Bq dm^{-3} in Table IIb.

For the calculation of the mean steady-state radon activity of Table IIb of 7.2 ± 0.6 Bq dm^{-3}, we omitted the value of the first outlet. Including the first outlet, the mean would be 7.0 ± 0.9 Bq dm^{-3}. Using the radon activity of 7.2 Bq dm^{-3}, the ingrowth is calculated with eq 1. The result is represented by the dashed line in Figure 2. Radon ingrowth and steady state (eq 1) were used to calculate residence times of the interstitial water from the inflow boundary to the outlets. Pore velocities were derived from the residence times and the respective flow distances (Table IIa). From the constant-input flow rate, and assuming a homogeneous distribution of hydraulic conductivity and effective porosity in the sand, we expected constant pore velocities throughout the box. The experimental pore velocity scattered considerably, however, around a mean of 0.58 ± 0.15 m day^{-1}, and the first two values were significantly higher than the others. The pore velocities obtained with the radon method were compared with the results of the concomitant NaCl tracer test.

Table III. Interpretation of Results from NaCl Tracer Test

outlet	distance x,[a] m	breakthrough $\bar{t}$,[b] days	breakthrough $\bar{v}$,[c] m day^{-1}	elution $\bar{t}$,[b] days	elution $\bar{v}$,[c] m day^{-1}
1	0.51	1.1	0.46	1.3	0.40
2	1.1	2.2	0.50	2.5	0.44
3	1.9	3.5	0.54	4.1	0.46
4	2.7	5.0	0.54	5.8	0.47
5	3.3	6.6	0.50	7.0	0.47
6	3.7	7.4	0.50	7.8	0.47
8	4.5	9.1	0.49	9.6	0.47
mean			0.50 ± 0.03		0.45 ± 0.03

[a] x, distance from inflow boundary. [b] $\bar{t}$, time at which C/C_0 = 0.5; see text. [c] $\bar{v} = x/\bar{t}$, pore velocity.

Tracer Test. In experiment i, the NaCl solution was injected synchronously with the Rn measurements during 274 h, beginning with a step stimulus. This tracer test gave an independent determination of the water residence times and allowed examination of the results of the radon measurements. The concentration–time distributions of the tracer were monitored in all outlets except outlet 7, which could not be monitored because of malfunction of the electric conductivity probe (Figure 4). At the breakthrough phase of the test, the NaCl tracer needed 9.1 days (mean residence time) to reach the most distant outlet, 8 (Table III). We define the mean residence time, $\bar{t}$, between the inflow boundary and the respective outlet of the

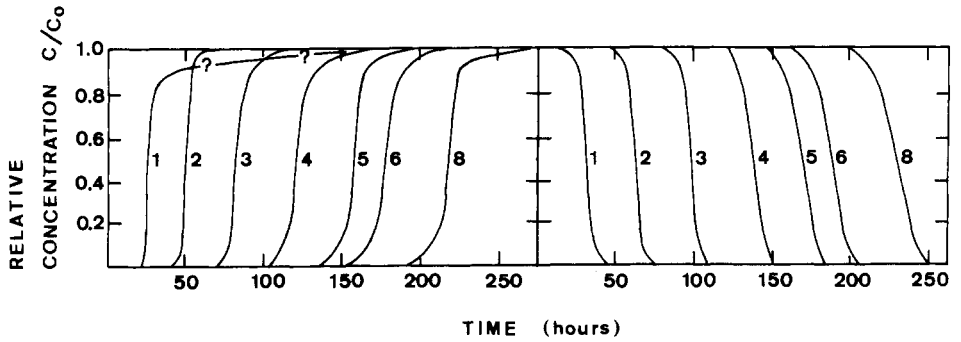

Figure 4. Breakthrough of NaCl tracer in box, C_0 = 200 ppm NaCl: left, breakthrough phase, right, elution phase; time starting at begin of injection of NaCl, and at begin of elution phase.

Table IV. Grain-Size and Activity Distributions of the Quartz Sand in the Box

grain-size fraction, μm	fractional wt, %	activity,[a] Bq kg^{-1}	fractional activity, %	grain surface area per dm^3,[b] m^2	Rn emanating power, 2.5 r^{-1},[b] μm^{-1}	fraction of emanating Rn,[c] %
<63	0.25	90	1.3	100	>0.17	>9
63–125	0.75	350	14.7	35	0.056	34
125–250	13	40	29.2	16	0.025	31
250–500	64	12	43.1	8	0.0125	22
500–1000	22	9.5	11.7	4	0.007	3

[a] Estimated from ^{214}Pb and ^{214}Bi γ-rays (*8*). [b] For spheres (cubic packing) of radii, r, of 15, 45, 100, 200, and 375 μm, for grain-size fractions of <63, 63–125, 125–250, 250–500, and 500–1000 μm. [c] Fractional activity times Rn emanating power.

water as the time at which 50% of the input NaCl concentration was reached (C/C_0 = 0.5). Subsequent to the continuous injection, tracer was flushed out of the box. At the elution phase of the test, the NaCl tracer needed 9.6 days to reach outlet 8, and background concentrations were attained after ~11 days. This is slightly less than the 13 days predicted by Darcy's law. The difference between measurement and calculation might be due to a wash-out of fine particles during earlier experiments, which may have increased the hydraulic conductivity compared to the measurement of Table I made during the initial packing of the box. Figure 4 shows the small spreading of the tracer with increasing flow distance during breakthrough and elution. The spreading is interpreted as diffusion and longitudinal dispersion, characterized by the dispersion coefficient, D_l (e.g., refs 5 and 6). The extended trailing edge of the breakthrough curve of outlet 1 cannot be explained. The longitudinal dispersion coefficient, estimated from the advection–dispersion equation (ADE; see below) and the measured NaCl breakthrough (Figure 4), resulted in a value of 0.035 m^2 day.$^{-1}$ This value indicates a very small influence of dispersion on tracer transport in this homogeneous sand.

Values of $\bar{t}$ are given in Table III, together with the respective pore velocities of the water, $\bar{v}$. Variations of the pore velocity may be due to a slightly inhomogeneous distribution of the sand-sized grains, which occurred during the packing of the box. The pore velocity calculated from the tracer breakthrough was 0.50 ± 0.03 m day.$^{-1}$ The elution phase of the test revealed ~10% lower pore velocities than the breakthrough phase, which agreed within errors. During the time of the test, the discharge rate of the pump varied by less than 3%. All experiments were performed at the same pore velocities. Unfortunately, other pore velocities were not feasible: A faster flow rate would have led to smaller fractions of radon ingrowth. A slower flow rate, though leading to a steady-state radon activity within the box, could yield erroneous results because of the large volume of samples withdrawn relative to the water entering the sand box.

The flow velocities estimated from the radon activities (Table IIa) are compared with those estimated from the NaCl tracer breakthrough (Table III): The NaCl values during the tracer breakthrough phase are of special interest because they were obtained synchronously with the radon experiment i. The radon values are based on eq 1, with a steady-state activity of 7.2 Bq dm^{-3} and an assumed homogeneous distribution of radium in the sand, while the NaCl tracer test values are based on the observation of the tracer's breakthrough. The first three values for the pore velocity of Table IIa are significantly higher than those of Table III. If the assumptions for the radon method are valid, an exponential ingrowth of radioactivity during experiment i should occur, after subtraction of the background activity of 0.11 Bq dm^{-3} of the inflowing water. We found activities at the first three outlets which were somewhat lower than those predicted with eq 1 (see Figure 2). A possible reason for the three low radon activities and related seemingly high pore velocities could be an inhomogeneous distribution of radium in the sand. We explore this assumption in the next section. The mean pore velocities resulting from the radon method of 0.58 ± 0.15 m day^{-1} and from the NaCl tracer test of 0.50 ± 0.03 m day^{-1} are, however, in agreement.

Distribution of ^{226}Ra in Size Fractions of Sand. The radon method assumes a homogeneous distribution of ^{226}Ra in the box. Surbeck (*8*) measured the activity of the γ-ray emitting radon daughters ^{214}Pb and ^{214}Bi in different grain-size fractions of the quartz sand (Table IV). The activity of these radon daughters corresponds to that of ^{226}Ra, if radon losses from the bulk grains are considered to be negligible, an assumption which is probably not correct for the <63-μm grains. The measurements indicated that the activities are highest in the fine fraction (<125 μm) of the sand, which contributes only 1% to the total mass.

Assuming that ^{226}Ra is distributed uniformly in the grains and that all grains are spheres of a given size, the recoil escape probability can be estimated (*7*) to be ~2.5 r^{-1}, where r is the grain radius. These assumptions are approximations due to aggregations of grains and preferential accumulation of specific minerals in certain grain fractions. The recoil escape probability, or the emanating power, is the contribution to radon release by direct α-

particle recoil. The recoil range for radon in minerals and rock materials is ~40 nm (7). Therefore, only the outermost part of the grains contributes to radon release by this mechanism and is thus roughly proportional to the surface/volume ratio of the grains. Estimations of grain surface area and radon emanating power are shown in Table IV, assuming that the calculated proportionality holds also in reality. From these estimations it is seen that grains of the size of <63 μm contribute ~10% and those of <125 μm more than 40% to the emanation of radon in this sand.

Prior to the radon experiments reported here, extended hydraulic experiments had been run in the box at much higher flow rates. During these earlier experiments, fine-grained material could have been transported from sections near the inflow boundary of the box to more distant domains. If fine particles are moved by the operation of the box, an inhomogeneous distribution in the radon activities could result, which could explain the observed deviations from an exponential ingrowth of ^{222}Rn.

Modeling Inhomogeneous Radon Production. We found that the simple approach of eq 1 did not account sufficiently well for the slightly nonexponential ingrowth of radon in the flowing water of the sand box. We do not known the real reason for the deviation of the observed data from the simple theory. To model the ingrowth of radon at conditions of an inhomogeneous production, we start from the stationary form of the ADE:

$$D_1 \frac{d^2A}{dx^2} - \bar{v} \frac{dA}{dx} - \lambda A + \gamma(x) = 0 \qquad (2)$$

where x is the distance along the flow direction.

The following relation allowed for a distance-dependent production rate, γ(x):

$$\gamma(x) = g_1 - [g_2 \exp(-g_3 x)] \qquad (3)$$

This relation approaches a constant value at greater distances. The constant g_1 is the far-distant production rate and is identical to the value used in eq 1 for the calculation of the residence time, assuming a homogeneous steady-state production rate of 7.2 Bq dm^{-3}. The constants g_2 and g_3 estimate the inhomogeneity. They were determined by fitting the experimental production rate at steady state (heavy line in Figure 3). The resulting values were g_2 = 5.0 Bq dm^{-3} and g_3 = 1.8 m^{-1}. From eq 3, $g_1 - g_2$ yields the activity at zero distance. The boundary conditions are

$$A(x=0) = 0 \qquad dA/dx(x=\infty) = 0$$

The resulting radon ingrowth is

$$A(x) = g_1/\lambda\,[1 - \exp(h)] - g_2/(\lambda - \bar{v}g_3 - D_1 g_3^2)\,[\exp(-g_3 x) - \exp(h)] \qquad (4)$$

where

$$h = \{[\bar{v} - (\bar{v}^2 + 4\lambda D_1)^{1/2}]x\}/2D_1$$

According to the NaCl experiment, the pore velocity was $\bar{v}$ = 0.5 m day^{-1} and the longitudinal dispersion coefficient was D_1 = 0.035 m^2 day^{-1}. The resulting ingrowth using eq 4 is represented by the solid line in Figure 2. A similar analysis, neglecting dispersion, showed a practically identical curve for the given set of parameters. For small distances, better agreement with the measurements is obtained with the inhomogeneous production (eq 4) than with the homogeneous production (eq 1). For larger distances, eq 1 shows better agreement. Note that an inhomogeneous production of radon, resulting from a heterogeneous distribution of radium in the sand, usually cannot be calculated in field experiments, because the local steady-state radon activities cannot be measured.

Conclusions

The results of the laboratory experiment confirmed the observations of our field studies in several porous aquifers of coarse gravel (*1*): The ingrowth of radon upon infiltration of surface waters to aquifers is mainly governed by the laws of radioactive decay. To simulate the radon transport in the box further, we used a term for a distance-dependent radon production. The rationale for the nonconstant radon production was the possibility to take into account an apparent inhomogeneous emanation of radon from the sand. Such inhomogeneities almost certainly occur in systems of infiltrating rivers: In the interstitial water of river-bed sediments, a faster increase of radon can be expected with distance than in the aquifer because of a higher content of fine-grained material in the river sediments. However, in the light of the overall errors of the method (±20%), the more sophisticated approach may not be justified for field investigations. Furthermore, the determination of the inhomogeneity by fitting parameters may not be possible under field conditions.

While the steady-state radon activity of the water in the box was found to be at ~7.2 Bq dm^{-3}, those of the groundwaters investigated at Swiss field sites amounted to 17–22 Bq dm^{-3}. The differences between the two systems may be due to the occurrence of Ra-containing sheet silicates (clays and micas) in natural geological materials and to the abundance of small particles with high surface area from which Rn can easily escape. The smaller steady-state value in the box experiment proved to be sufficient for the estimation of residence times and pore velocities. The pore velocities obtained in this experiment with the radon method agreed with those deduced from a NaCl tracer test. They were ~10 times smaller than groundwater flow velocities observed at Swiss field sites (*1*), but are of the same order of magnitude as flow velocities of sandy aquifers, e.g., that investigated at Chalk River, Canada (*2*). There, the aquifier consists of sand similar to that in our box experiment.

Acknowledgments

We thank H. Surbeck for radioactivity measurements on the sandy material of the box, E. Rössler for drafting Figure 4, and R. Lorenzen for finalizing the manuscript. The constructive comments of the anonymous reviewers are acknowledged.

Registry No. ^{222}Rn, 14859-67-7.

Literature Cited

(1) Hoehn, E.; von Gunten, H. R. *Water Resour. Res.* **1989**, *25*, 1795.
(2) Pickens, J. F.; Jackson, R. E.; Inch, K. J.; Merritt, W. F. *Water Resour. Res.* **1981**, *17*, 529.
(3) Stauffer, F.; Dracos, Th. *J. Hydrol.* **1986**, *84*, 9.
(4) Horiuchi, K.; Murakami, Y. *Chem. Lett.* **1979**, 442.
(5) Pickens, J. F.; Grisak, G. E. *Water Resour. Res.* **1981**, *17*, 1191.
(6) Bear, J. *Hydraulics of Groundwater*; McGraw-Hill Inc.: New York.
(7) Andrews, J. N.; Wood, D. F. *Trans.—Inst. Min. Metall., Sect. B* **1972**, *81*, B198.
(8) Surbeck, H. personal communication, 1988.
(9) Adank, P. personal communication, 1987.

Received for review July 2, 1991. Revised manuscript received November 21, 1991. Accepted November 26, 1991. Work partly funded by the Swiss National Science Foundation.